

Solvent Responsive and Switchable Nanofiltration Membranes based on Hypercrosslinked Polymers with Permanent Porosity

Kai Schute,^[a] Felicitas Jansen,^[a] and Marcus Rose^{[a,b]*}

Abstract: Porous organic framework materials such as hypercrosslinked polymers (HCP) show a high chemical stability and dynamic behavior in a variety of solvents while their pore properties exhibit a great potential for mixed matrix membrane (MMM) applications. However, their influence as porous filler in MMMs, especially for applications in the liquid phase filtration is still unexploited. Herein, we demonstrate the first HCP-based MMM for molecular separation in the liquid phase by nanofiltration (NF). In dependence of the solvent, the membrane changes its fractional free volume by shrinking or swelling. Connected to that also the pore size is influenced, hence, providing a tunable permeance and molecular cut-off. The reduction of the pore volume and size directly correlates to the improvement of the NF performance while the volume increase completely diminishes it. The extraordinary flexibility and high degree of crosslinking assure permanent porosity and render the dynamic behavior fully reversible. Thereby, a solvent responsive on- and off-switching of the NF properties is enabled and was experimentally proven. Overall, this provides novel strategies regarding the fouling and regeneration of membranes as well as the inhibition of pore blocking in membrane-derived processes by a tunable separation performance.

Introduction

Molecular separation by nanofiltration (NF) in either aqueous or organic media has emerged to a highly promising purification technology.^[1] However, the greatest challenge is still to overcome the trade-off between permeability and selectivity in order to reach higher efficiencies. One solution is the development of membranes based on innovative materials such as metal-organic frameworks (MOFs), zeolitic imidazolate framework (ZIFs) or porous aromatic frameworks (PAFs).^[2] Their defined and adjustable pore properties as well as their exceptionally high structural variety might enable to address the trade-off challenge. Especially the concept of mixed-matrix membranes (MMM) raised a great interest as the simple processability of the aforementioned non-soluble materials became feasible.^[3] In general, the MMM approach is typically based on a continuous non-porous polymer phase while the

desired performance material is embedded as a filler. So far, many studies on MMM tend to focus on applications in gas separation in which the performance could be significantly enhanced. Other membrane-based separations mainly in the liquid phase such as solvent-resistant nanofiltration (SRNF) or pervaporation (PV) have been investigated as well^[4] although they are typically limited by the poor stability of either the filler or the matrix in contact with the organic liquid.^[5] As most materials tend to swell significantly under those conditions pore channels are widened and result in an increased permeability and decreased selectivity and hence, affects the long term stability. This lack of stability even becomes more relevant for aqueous solutions. Especially the majority of MOFs are poorly stable in the presence of water and their pore structure collapses.^[6] Just very recently a few studies report first investigations on aqueous media; however mostly on a conceptual level.^[7] To tackle the stability issue of MOFs as fillers microporous polymer networks are promising alternative materials.

Hypercrosslinked polymers (HCP) are among the most investigated porous polymers and organic framework materials because they offer a permanent microporosity with specific surface areas as high as 2000 m²g⁻¹ and a convenient synthesis route.^[8] Typically, they are produced by Friedel-Crafts alkylation either with an internal or an external electrophile resulting in exceptional high crosslinking degrees. Also, their porosity is influenced not only by the geometry of the building block and the crosslinking degree but also by the function of the applied solvent as porogen. Very recently, the team of Cooper et al. reported for the first time a HCP-based MMM with PIM-1 (polymer of intrinsic microporosity) as matrix polymer and stated them to be a remarkably cheap and effective nanofiller to enhance the selectivity in gas separation applications.^[9] Thereafter, the group of Wood et al. applied HCP as filler in a poly(1-trimethylsilyl-1-propyne) (PTMSP) matrix.^[10] Thereby, they improved the transport performance and the selectivity for the separation of CO₂/N₂ gas mixtures. They were also able to minimize ageing effects of the membranes which is a common problem for high fractional free volume materials such as PTMSP or PIM-1. These two studies already revealed the high potential of HCPs as porous additive in MMMs although the question what the reason for this improvement is remains yet unanswered. The following three mechanisms are probably involved and responsible also for the selectivity: I) solution-diffusion in the matrix polymer, II) Knudsen diffusion in the porous filler, and III) adsorption and surface diffusion in the porous filler. However, it is expected that as for MOF-MMMs the surface interaction of the filler particles with the matrix polymer is crucial since this interface is involved in the mass transfer. Hence, it seems feasible that especially the interaction of a porous organic polymer filler with a matrix polymer significantly enhances the separation performance due to the similar chemical nature compared to less attractive interactions with

[a] K. Schute, F. Jansen, Prof. Dr. M. Rose
Institut für Technische und Makromolekulare Chemie
RWTH Aachen University
52074 Aachen, Germany

[b] Prof. Dr. M. Rose
Ernst-Berl-Institut, Technische Chemie II
Technische Universität Darmstadt
64287 Darmstadt, Germany

* Corresponding author: rose@tc2.tu-darmstadt.de

Supporting information for this article is given via a link at the end of the document.

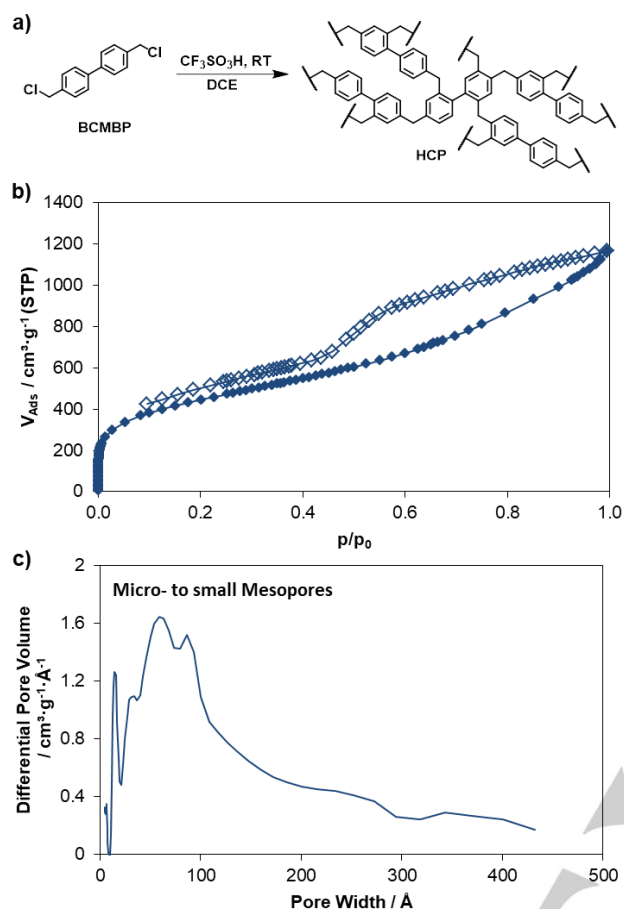


Figure 1 a) Reaction scheme of the synthesis of the BCMBP-based HCP. b) N_2 physisorption isotherm measured at 77 K. c) Differential pore size distribution determined by DFT method.

inorganic or hybrid filler materials. Additionally, since HCPs typically contain micro- as well as small mesopores a good separation performance is expected rather for organic molecules with molecular weights in the order of magnitude of 100 g mol^{-1} than for small gas molecules. Therefore, exploiting the potential of HCPs as fillers for MMM for alternative applications such as liquid phase nanofiltration is crucial to facilitate further development of innovative membrane materials.

In this work, we report the production of HCP-based MMM and, to our knowledge for the first time, applied them for molecular separation in the liquid phase. Aqueous phase nanofiltration of different dye molecules reveals the range of molecular cut-off and the importance of the non-polar surface chemistry of the HCP filler. During regeneration of the membrane with organic solvents the swelling and shrinking behavior is found to be fully reversible. A detailed investigation reveals the flexibility and the dynamic behavior of the HCP-MMM. Hence, they enable a solvent-responsive permeance and retention. This unique effect might not only be useful to tune the separation performance but also to enable efficient membrane regeneration after fouling.

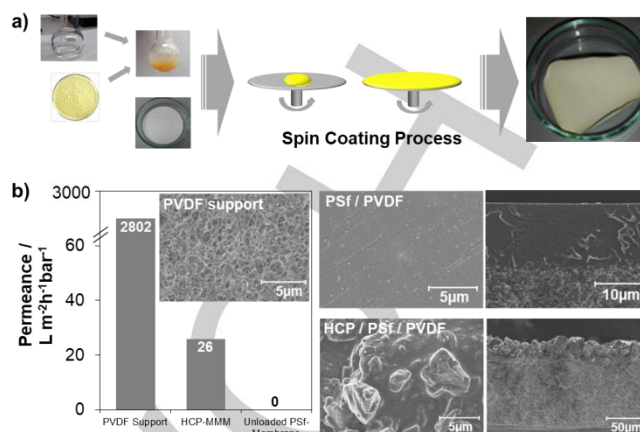


Figure 2 a) Schematic representation of the general membrane preparation by spin coating. b) initial permeance of the PVDF support, the HCP-embedded MMM (40 wt-%) and the unloaded PSf coated membranes together with the corresponding SEM images from the top (left) and cross-sectional (right) perspective, respectively.

Results and Discussion

The HCP was synthesized using a novel strategy which was recently published by our group using the aromatic and bifunctional 4,4'-bis(chloromethyl)biphenyl (BCMBP) as the building block and trifluoromethanesulfonic acid for initiation of the metal-free crosslinking reaction.^[11] The material showed a broad pore size distribution with a very high degree of micro- to small mesopores (the majority below 10 nm) as determined by N_2 -physisorption and DFT data evaluation (Figure 1). These pore diameters are typically required in order to create a reasonable molecule rejection for aqueous NF applications. The corresponding specific BET surface was calculated with a value of $1842 \text{ m}^2 \text{ g}^{-1}$.

Different amounts of the HCP particles were dispersed in a 20 wt-% solution of polysulfone (PSf) in dimethylformamide (DMF), immediately increasing the viscosity of the dispersion. PSf was chosen as matrix polymer, as it creates a dense, glassy matrix, impermeable for liquid solvents if dried slowly in order to reach its equilibrium state.^[12] Furthermore, the aromatic units of the PSf were assumed to positively interact with the aromatic HCP to avoid undesired macroreticulate voids between the binder and filler polymer. After sonication the homogenized suspension was then coated on a PVDF microfiltration support membrane via spin-coating and dried (Figure 2a). For the HCP/PSf membrane it was quite important to find the optimal loading of HCP and film thickness to guaranty a suitable processability, which became more difficult with a higher HCP loading, together with a high permeance as shown later. Screening these parameters exhibited an increase in the permeance of water with a higher loading of the porous polymer (Figure S1). Obviously, the porous polymer adds permeable pore channels into the non-permeable matrix membrane. The ideal balance of flux and processing was found to be with a high loading of 40 wt-% HCP compared to the amount of PSf used and a spinning rate of 10'000 rpm. The compared permeances

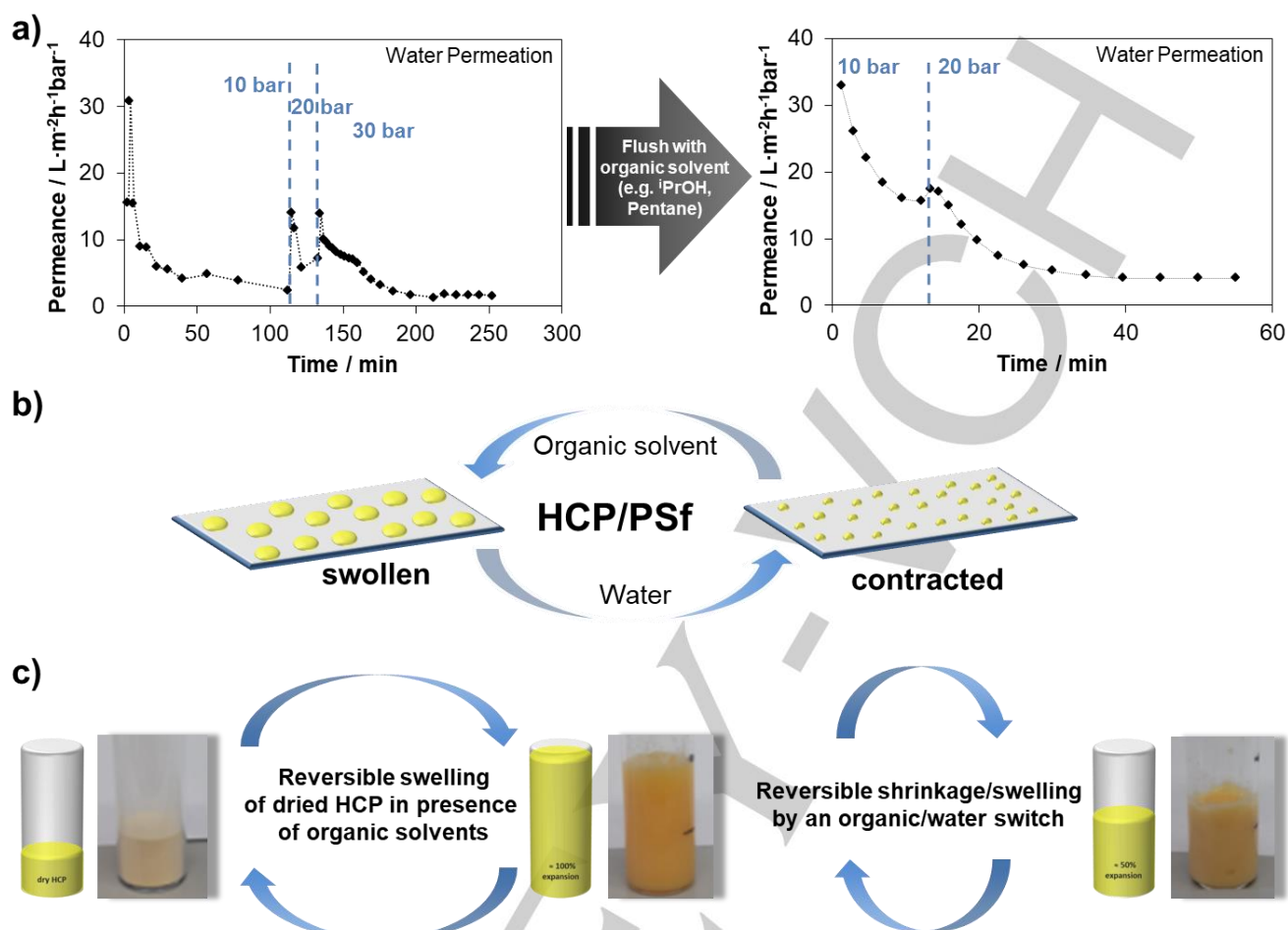


Figure 3. a) Behavior of the permeance of water over time and after purging with an organic solvent for the HCP/PSf MMM (40 wt-%) (note: the pressure increases refer to an increase of the transmembrane pressure from 10 to 20 to 30 bar during the dead end experiment in order to still enable a reasonable high water flux); b) Illustration of the HCP embedded particles swelling and shrinking by a solvent change; c) Depiction of the macroscopic volume change of HCP in water and organic solvents.

of the PVDF support ($2802 \text{ L m}^{-2} \text{ h}^{-1} \text{ bar}^{-1}$), the unloaded PSf membrane with a film thickness of $9 \mu\text{m}$ (until 60 bar after 120 min; $0 \text{ L m}^{-2} \text{ h}^{-1} \text{ bar}^{-1}$) and the HCP/PSf MMM with a comparable thickness (40 wt-%) ($26 \text{ L m}^{-2} \text{ h}^{-1} \text{ bar}^{-1}$) are presented in Figure 2b.

SEM micrographs revealed a homogeneous dispersion of the HCP particles in the PSf matrix (Figure 2b, S2 and S3). The overall film thickness is mainly determined by the particle size of the porous polymer. Fully embedded HCP particles are proven by SEM and IR (Figure S3 and S4). The electron micrographs exhibit no macrovoids and thus, confirm the good compatibility of the matrix and the porous filler polymers. Furthermore, the ability for solvent permeance through the PSf matrix could be excluded as permeance experiments of the unloaded PSf ($9 \mu\text{m}$ thickness) show no flux within the tested pressure range (0–60 bar, Figure 2b).

Investigation of the water permeance revealed an unexpected behavior of the HCP/PSf MMM. With increasing time of operation, the water permeance decreased significantly from $30.8 \text{ L m}^{-2} \text{ h}^{-1} \text{ bar}^{-1}$ until it levelled off at a constant value of $1.9 \text{ L m}^{-2} \text{ h}^{-1} \text{ bar}^{-1}$ (Figure 3a). Initially, we assumed an irreversible

ageing of the membrane as it is commonly known for high free volume polymers such as PTMSP or polymers of intrinsic microporosity (PIM).^[13] However, if the MMM was exposed to an organic solvent, such as *iso*-propanol or *n*-pentane, the permeance could be increased significantly (Table S2). If switched back to water, the observed permeance behaved comparable to the fresh HCP/PSf membrane, though the equilibrated state was reached after a shorter period of time. Accordingly, irreversible ageing could not be the cause. As PSf is commonly known to be quite unaffected by these organic solvents, we assumed a flexible behavior of the pore system of HCP to be responsible for this behavior. To further proof this hypothesis pure HCP powder was exposed to organic solvents (Figure 3c). Hence, severe swelling was observed by a volume increase of about 100% compared to the initial volume, respectively, increasing the polymers pore volume and pore size. If exchanged to water, the polymer immediately shrunk (about 50%) and thereby decreasing the accessible pore volume. Additionally, water vapor adsorption also showed an extraordinary repellent effect of the HCP for water (Figure S6). Comparing the vapor uptake with a commercial activated carbon

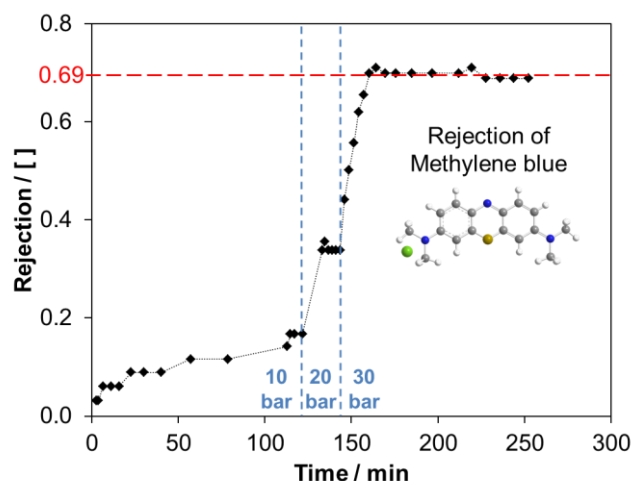


Figure 4. Time and pressure (10 to 20 to 30 bar) dependent rejection of methylene blue by the HCP-loaded mixed matrix membrane (40 wt %).

as a general reference material the HCP showed an extremely low adsorption capacity, indirectly stating the repulsive properties of the porous polymer for water. Conveying this observation to the mixed matrix membrane, this swelling and shrinking of the pore system depending on the solvents polarity will also occur on a much smaller level inside the MMM explaining the observed changes in the permeance. A somewhat similar behavior was also observed by Woodward et al. during gas sorption studies on HCP, further proving the hypothesis.^[14] However, it is noteworthy that HCP maintains its permanent porosity due to the high crosslinking degree. Hence, despite severe shrinking, a certain pore volume and size remains intact and enables constant permeation after reaching steady state conditions concerning the dynamic behavior of the polymer.

Based on this dynamic behavior depending on the degree of swelling or shrinking and hence, a variable pore size, the rejection performance of the HCP MMMs was investigated. As the pore size distribution of HCP determined from nitrogen physisorption by a DFT model exhibited a broad distribution from micro- to small mesopores (majority below 10 nm), and thereby in the range of small to medium sized molecules, we chose methylene blue (MB) as a commonly used dye, for the initial rejection studies. With a molecular weight of 319.7 g mol^{-1} it is a suitable dye for testing the NF performance of the respective membrane. The experiment was carried out using the 40 wt-% loaded HCP/PSf mixed matrix membrane (Figure 4). Initially, the overall rejection of methylene blue was negligible (0.03). However, over time the rejection of methylene blue increased. This correlates with the changing permeance of water by shrinking of the pore system and hence, reduction of the pore size (Figure 3a). As in the previous experiments the pressure was increased in two steps from 10 to 20 and then to 30 bar. Since this enabled initially a higher flux but also a more severe pore shrinking, the retention of methylene blue increases drastically to 0.34 after 120 min and reaches even 0.69 after 160 min. Keeping the pressure constant enables a constant retention of methylene blue without further changes in the

investigated time range. If compared to the water permeance, which indirectly indicates the pore shrinking, the equilibrated

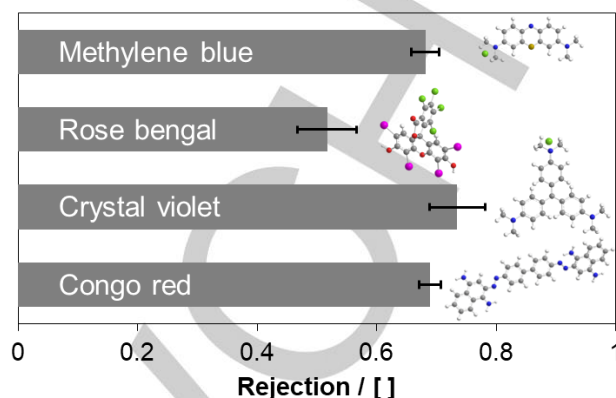


Figure 5. Rejection of different dyes in H_2O for the HCP/PSf MMM (40 wt %).

state was reached, thereby expecting no further changes of the rejection. During testing, the nanoporous HCP initially shows no NF performance as still a high fraction of pores are large enough for the dye to pass the pore channels resulting in no observable rejection. With further shrinking of the pore system, also due to the two pressure steps, the pore diameter decreases as much to observe a significant rejection of the dye molecules. It should also be mentioned, that adsorption processes of the dissolved dye, which tend to occur in high surface area materials as the HCP or in porous materials in general are not responsible for the rejection as the NF performance is directly correlating to the pressure behavior and the water permeance. If adsorption would have been responsible for the observed concentration change between feed and permeate the rejection should have decreased over time, due to reaching the maximum adsorbed amount. This was not observed over several hours of testing.

To further investigate the NF performance of the HCP/PSf membrane different dyes were tested (Figure 5, S5). They differ in their molecular weight as well as in their polarity. Interestingly, it could be noted that the ionic dyes methylene blue, crystal violet (CV) and congo red (CR) showed a rejection in the same range even though their molecular weights were different (Table S1). Apparently, not only a molecular sieving effect is responsible but also an influence of the molecules polarity in combination with the broad pore size distribution of HCP. More strikingly however, was the rejection of only 0.52 observed for rose bengal (RB). Of the selected dyes it is the heaviest and bulkiest due to the large iodine groups and the very low rotational flexibility. However, RB showed the lowest rejection of the tested dyes. It is non-ionic and though, the molecule with the lowest polarity. As vapor adsorption and swelling tests already showed, HCP has a greater affinity towards molecules with a lower polarity. Hence, the same conclusion refers to the MMMs rejection characteristics. Besides the size exclusion effect of the membrane a polarity-directed effect needs to be taken into account as well as the impact of the dissolved species that influences the polarity of the solution and hence, also the swelling/shrinking behavior.

Besides the general trade-off between permeance and selectivity membrane fouling is another effect which generally tends to occur in membrane processes due to pore blocking.^[15] Approaches to avoid or reverse fouling are usually back-flushing or the use of additives. These procedures are often unwanted and typically decrease the life span of a membrane significantly. The remarkable flexibility of HCP in the membranes reported herein could therefore enable an improved strategy to avoid fouling using the switchable pore swelling/shrinking behavior of the HCPs pore structure. Therefore, we tested the HCP/PSf membrane under different solvent conditions. After equilibrating the membrane we conducted rejection studies for all the dyes in organic media, specifically in iso-propanol and n-pentane (Table S2). We immediately observed an enhanced permeance for the respective solvents while no rejections were observed for all tested dyes due to the increased pore diameter and lower polarity of the medium. If the solvent was changed back to water the initial degree of swelling/shrinking of the HCP together with the former rejections were obtained again. Hence, the change of the pore structure, depending on the solvent is proven to be reversible. To our knowledge such an observation was not yet explicitly mentioned in membrane processes. Thus, this provides a strategy against fouling in membrane separations by simply switching the pore size through a reversible solvent change. Potentially blocked pores by small molecules, at least in the case of NF processes, could thereby be unblocked and the membrane permeance, often decreased by fouling, would be restored while the integrity of the HCP/PSf MMM remains intact.

Conclusions

In conclusion, we developed a mixed matrix membrane using a BCMBP-based hypercrosslinked polymer as a nanoporous filler which showed optimal matrix-filler-interactions with the used matrix polymer polysulfone. For the first time we investigated such HCP-based membranes in liquid nanofiltration with a special focus on aqueous media. Using a set of different dyes we demonstrated the NF performance with rejection of molecules in the size of dyes such as methylene blue. The HCPs flexibility and solvent affinity were identified to be the crucial properties to enable a significant molecular rejection. Exchanging the solvent resulted in variations of the pore size of the porous filler depending on whether the medium is aqueous and organic and hence, depending on the solvents polarity. These changes are fully reversible and thus, enable a strategy against membrane fouling during nanofiltration by enlarging and reducing the average pore diameters of the porous filler material.

Experimental Section

HCP synthesis

To a solution of 1.0 g (3.98 mmol) of 4,4'-bis(chloromethyl)biphenyl (BCMBP; Aldrich) dissolved in 10 mL of 1,2-dichloroethane (DCE; Aldrich), 0.9 g (5.97 mmol) of trifluoromethanesulfonic acid (CF₃SO₃H)

(Fluorochem) was added dropwise. The solution immediately changed color from colorless via blue to black, while a solid was formed until no further agitation was possible. Afterwards, the mixture was kept under ambient conditions for an additional hour to increase the degree of crosslinking. The obtained monolithic solid was reduced to small pieces, washed with ethanol and de-ionized water and filtered off to obtain a yellow solid after drying.

Membrane preparation

In order to obtain the HCP/PSf mixed-matrix membranes (MMM), a solution of a 20 wt-% polysulfone (PSf; av. $M_w = 20.000 \text{ g mol}^{-1}$; Aldrich) in dimethylformamide (DMF; Aldrich) was prepared. Different amounts of finely grinded BCMBP-based HCP (particle size < 50 μm) (19, 25, 30, 40 wt-% with respect to the amount of polymer) was added to the polymer solution and intensively suspended. The suspensions viscosity increase significantly after a few minutes, due to the materials swelling until no further agitation was possible. The suspension was then sonicated for an hour in an ultrasonic bath to allow further homogenization and to remove any remaining air. Afterwards, the fine dispersion was poured on a PVDF microfiltration membrane support (Merck Millipore Durapore®; pore size 0.22 μm) and coated via the spin coating technique at different rotating velocities (8000, 9000, 10000 rpm). The coated support was slowly dried at ambient conditions for at least 48 h because of the low vapor pressure of DMF and to achieve the fully equilibrated and dense state of the PSf matrix to minimize potential defects.

Analytical methods

Textural properties were characterized by nitrogen physisorption measurements. All experiments were performed at 77.4 K using a Micromeritics ASAP 2000 physisorption analyzer. The porous HCP was degassed under vacuum at 120 °C for 12 h before the measurement. The pore size distribution was determined using the implemented DFT model in the MicroActive software (Micromeritics): NLDFT, N₂, 77 K, solid surfaces of all materials (<http://www.micromeritics.com/library/DFT-NLDFT-Density-Functional-Theory/NLDFT-DFT-Models.aspx>).

Attenuated total reflectance infrared-spectra (ATR-IR) were measured using a Vertex 70 from Bruker. Measurements were carried out from 400-2500 cm^{-1} with 64 scans.

Scanning electron microscopy studies were conducted using a Jeol JSM-7000F SEM microscope equipped with a field emission cathode and a maximum lateral resolution of 1.2 nm at 30 kV.

Membrane characterization

The membranes were tested in a dead-end filtration set up with a maximum applied pressure of 60 bar (Sterlitech HP 4750 stirred cell). Permeance tests were conducted either with water, iso-propanol or n-pentane at different pressures due to variations in the permeance behavior of each membrane. The active membrane area was 14.6 cm^2 and the permeance ($\text{L m}^2 \text{ h}^{-1} \text{ bar}^{-1}$) has been determined according to the following equation:

$$P = V \cdot A^{-1} \cdot p^{-1} \cdot t^{-1}$$

where V (L) denoted the collected volume, p (bar) the applied pressure and t (h) the time of collecting.

All characterizations and quantifications of the nanofiltration performance were tested with the HCP/PSf MMM and a loading of 40 wt-%. Four different dyes (Aldrich) of different molecular weights and ionic properties were chosen in order to analyze the NF behavior (Table

S1). All aqueous dye solutions were prepared with a concentration of 0.015 mg g⁻¹. The feed and permeate concentrations were quantified by photometry and rejections were calculated according to

$$R=1-(C_p/C_f^{-1})$$

where C_p is the permeate concentration and C_f is the feed concentration.

Acknowledgements

We gratefully acknowledge financial support by the German Research Foundation (Grant No. RO 4757/2-1) and the Excellence Initiative of the German federal and state governments.

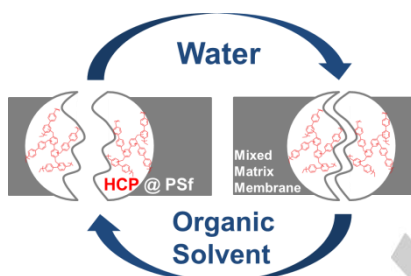
Keywords: porous polymer, organic framework, superhydrophobic surface, stimuli-responsive material, nanofiltration membrane

- [1] Selected Reviews: a) A. Lee, J. W. Elam, S. B. Darling, *Environ. Sci.: Water Res. Technol.* **2016**, *2*, 17-42; b) A. G. Fane, R. Wang, M. X. Hu *Angew. Chem. Int. Ed.* **2015**, *54*, 3368-3386; *Angew. Chem.* **2015**, *127*, 3427-3447; c) P. Vandezande, L. E. M. Gevers, I. F. J. Vankelecom, *Chem. Soc. Rev.* **2008**, *37*, 365-405; d) A. W. Mohammad, Y. H. Teow, W. L. Ang, Y. T. Chung, D. L. Oatley-Radcliffe, N. Hilal, *Desalination*, **2015**, *356*, 226-254; e) P. Marchetti, M. F. Jimenez Solomon, G. Szekely, A. G. Livingston, *Chem. Rev.* **2014**, *114*, 10735-10806.
- [2] a) A. F. Bushell, P. M. Budd, M. P. Atfield, J. T. A. Jones, T. Hasell, A. I. Cooper, P. Bernardo, F. Bazzarelli, G. Clarizia, J. C. Jansen, *Angew. Chem. Int. Ed.* **2013**, *52*, 1253-1256; *Angew. Chem.* **2013**, *125*, 1291-1294; b) S. Sorribas, P. Gorgojo, C. Téllez, J. Coronas, A. G. Livingston, *J. Am. Chem. Soc.* **2013**, *135*, 15201-15208; c) P. Gorgojo, S. Karan, H. C. Wong, M. F. Jimenez-Solomon, J. T. Cabral, A. G. Livingston, *Adv. Funct. Mater.* **2014**, *24*, 4729-4737; d) T. Rodenas, I. Luz, G. Prieto, B. Seoane, h. Miro, A. Corma, F. Kapteijn, F. X. L. I Xamena, J. Gascon, *Nature Mater.* **2015**, *14*, 48-55; e) M. F. Jimenez-Salomon, Q. Song, K. E. Jelfs, M. Munoz-Ibanez, A. G. Livingston, *Nature Mater.* **2016**, *15*, 760-769.
- [3] a) B. Soane, J. Coronas, I. Gascon, M. E. Benavidas, O. Karvan, J. Caro, F. Kapteijn, J. Gascon, *Chem. Soc. Rev.* **2015**, *44*, 2421-2454; b) Z. Wang, D. Wang, S. Zhang, L. Hu, J. Jin, *Adv. Mater.* **2016**, *28*, 3399-3405; c) Z. Qiao, S. Zhao, J. Wang, S. Wang, Z. Wang, M. D. Guiver, *Angew. Chem. Int. Ed.* **2016**, *55*, 9321-9325; *Angew. Chem.* **2016**, *128*, 9467-9471.
- [4] a) Y. Ying, Y. Xiao, J. Ma, X. Guo, H. Huang, Q. Yang, D. Liu, C. Zhong, *RSC Adv.* **2015**, *5*, 28394-28400; b) L. Zhu, H. Yu, H. Zhang, J. Shen, L. Xue, C. Gao, B. van der Bruggen, *RSC Adv.* **2015**, *5*, 73068-73076; c) Y.-H. Deng, J.-T. Chen, C.-H. Chang, K.-S. Liao, K.-L. Tung, W. E. Price, Y. Yamauchi, K. C.-W. Wu, *Angew. Chem. Int. Ed.* **2016**, *55*, 12793-12796; *Angew. Chem.* **2016**, *128*, 12958-12988; d) M. Shan, B. Seoane, E. Rozhko, A. Dikhtiarenko, G. Clet, F. Kapteijn, J. Gascon, *Chem. Eur. J.* **2016**, *22*, 1-5.
- [5] a) I. Soroko, Y. Bhole, A. G. Livingston, *Green. Chem.* **2011**, *13*, 162-168; b) K. Hendrix, M. van Eynde, G. Koeckelberghs, I. F. J. Vankelecom, *J. Membr. Sci.* **2013**, *447*, 212-221.
- [6] a) J. B. DeCoste, G. W. Paterson, B. J. Schindler, K. L. Killops, M. A. Browe, J. J. Mahle, *J. Mater. Chem. A.* **2013**, *1*, 11922-11932; b) Q. Yang, S. Vaesen, G. Ragon, A. D. Wiersum, D. Wu, A. Lago, T. Devix, C. Martineau, F. Taulelle, P. L. Llewellyn, H. Jobic, C. Zhong, C. Serre, G. De Weireld, G. Maurin, *Angew. Chem. Int. Ed.* **2013**, *52*, 10316-10320; *Angew. Chem.* **2013**, *125*, 10506-10510.
- [7] a) R. Zhang, S. Ju, N. Wang, L. Wang, G. Zhang, J. R. Li, *Angew. Chem. Int. Ed.* **2014**, *53*, 9775-9779; *Angew. Chem.* **2014**, *126*, 9933-9937; b) Y. Zhang, X. Feng, H. Li, Y. Chen, J. Zhao, S. Wang, L. Wang, B. Wang, *Angew. Chem. Int. Ed.* **2015**, *54*, 4259-4263; *Angew. Chem.* **2015**, *127*, 4333-4337; c) M. S. Denny, Jr., S. M. Cohen, *Angew. Chem. Int. Ed.* **2015**, *54*, 9029-9032; *Angew. Chem.* **2015**, *127*, 9157-9160.
- [8] a) S. Xu, Y. Luo, B. Tan, *Macromol. Rapid Commun.* **2013**, *34*, 471-484; b) N. Fontalas, R. M. Marce, F. Borrull, P. A. G. Cormack, *Polym. Chem.* **2015**, *6*, 7231-7244.
- [9] T. Mitra, R. S. Bhavsar, D. J. Adams, P. M. Budd, A. I. Cooper, *Chem. Commun.* **2016**, *52*, 5581-5584.
- [10] C. H. Lau, X. Mulet, K. Konstas, C. M. Doherty, M-A. Sani, F. Separovic, M. R. Hill, C. D. Wood, *Angew. Chem. Int. Ed.* **2016**, *55*, 1998-2001; *Angew. Chem.* **2016**, *128*, 2038-2041.
- [11] K. Schute, M. Rose, *ChemSusChem* **2015**, *8*, 3419-3423.
- [12] I. Pinnau, W. J. Koros, *J. Appl. Polym. Sci.* **1991**, *43*, 1491-1502.
- [13] C. L. Staiger, S. J. Pas, A. J. Hill, C. J. Cornelius, *Chem Mater.* **2008**, *20*, 2606-2608.
- [14] R. T. Woodward, L. A. Stevens, R. Dawson, M. Vjayaraghavan, T. Hasell, I. P. Silverwood, A. V. Ewing, T. Ratvijitvech, J. D. Exley, S. Y. Chong, F. Blanc, D. J. Adams, S. G. Kazarian, C. E. Snape, T. C. Drage, A. I. Cooper, *J. Am. Chem. Soc.* **2014**, *136*, 9028-9035.
- [15] W. Guo, H-H. Ngo, J. Li, *Bioresource Technol.* **2012**, *122*, 27-34.

Entry for the Table of Contents (Please choose one layout)

FULL PAPER

Mixed-matrix membranes based on nanoporous polymers with flexible networks and permanent porosity exhibit an adjustable permeation and rejection performance in liquid phase nanofiltration. The flexible pore system of the polymer network provides a fully reversible swelling/shrinking behaviour that is used to tailor the separation performance and enables strategies to reverse membrane fouling.



*K. Schute, F. Jansen, M. Rose**

Page No. – Page No.

Solvent Responsive and Switchable Nanofiltration Membranes based on Hypercrosslinked Polymers with Permanent Porosity

Additional Author information for the electronic version of the article.

Author: M. Rose ORCID identifier: 0000-0001-8196-1353

WILEY-VCH